

X-ray Images of Hot Accretion Flows

Feryal Özel¹ & Tiziana Di Matteo²

Harvard-Smithsonian Center for Astrophysics, 60 Garden Street, Cambridge, MA 02138;
fozel, tdimatteo@cfa.harvard.edu

ABSTRACT

We consider the X-ray emission due to bremsstrahlung processes from spherically-symmetric low radiative-efficiency hot accretion flows around supermassive and galactic black holes. We calculate surface brightness profiles and Michelson visibility functions for a range of density profiles, $\rho \sim r^{-3/2+p}$, with $0 < p < 1$, to allow for the presence of outflows. We find that although the 1 keV emitting region in these flows can always extend up to 10^6 Schwarzschild radii (R_S), their surface brightness profiles and visibility functions are strongly affected by the specific density profile. The advection-dominated solutions with no outflows ($p = 0$) lead to centrally peaked profiles with characteristic sizes of only a few tens of R_S . Solutions with strong outflows ($p \sim 1$) lead to flat intensity profiles with significantly larger characteristic sizes of up to $10^6 R_S$. This implies that low luminosity galactic nuclei, such as M87, may appear as extended X-ray sources when observed with current X-ray imaging instruments. We show that X-ray brightness profiles and their associated visibility functions may be powerful probes for determining the relevant mode of accretion and, in turn, the properties of hot accretion flows. We discuss the implications of our results for observations with the *Chandra* X-ray Observatory and the proposed X-ray interferometer *MAXIM*.

Subject headings: accretion, accretion flows – black hole physics – radiation mechanisms: thermal bremsstrahlung – galaxies: nuclei – X-rays: galaxies

1. Introduction

Imaging X-ray emitting regions around black holes addresses questions related both to black hole physics and to accretion phenomena. Depending on the properties and the extent of the X-ray emission as well as its proximity to the black hole, the X-ray images may have imprinted on them the accretion geometry, its physical properties, and even signatures of the space-time around the black hole. In standard models, the X-ray emission from active galactic nuclei (AGN) is assumed

¹Physics Department, Harvard University

²*Chandra* Fellow

to arise from a hot corona above a geometrically thin accretion disk. Thermal Comptonization of disk blackbody photons in the corona leads to the production of a hard X-ray continuum, some of which is reprocessed by the underlying disk (e.g., Haardt & Maraschi 1991, 1993). From the properties of the hard X-ray continuum and of the reflected component (e.g., Nandra et al. 1997) it is now established that the majority of X-ray emission from AGN originates from regions close to the black holes, corresponding to $\lesssim 3 - 20R_S$, where R_S is the Schwarzschild radius of the black hole.

In recent years it has become apparent that standard thin disk accretion with high radiative efficiency may not be common in nearby galaxies. The centers of most nearby galaxies also harbor supermassive black holes (e.g., Magorrian et al. 1998) but, unlike the more distant AGN, display little or no activity. It has been shown that the nuclei of nearby giant elliptical galaxies, which host the largest black holes known with masses of $10^8 - 10^{10}M_\odot$ (e.g., Magorrian et al. 1998), the center of the Milky Way with its $2.5 \times 10^6M_\odot$ black hole (e.g., Eckart & Genzel 1997), and even some of the galactic black hole sources like A0620 in quiescence are remarkably underluminous for their expected mass accretion rates. The relative quiescence and spectral characteristics of these sources can be explained if the central black holes accrete via low radiative-efficiency accretion flows or ADAFs (Rees et al. 1982; Fabian & Rees 1995; Narayan, Yi, & Mahadevan 1995; Narayan, McClintock, & Yi 1996; Di Matteo et al. 2000; for a review see, e.g., Narayan, Mahadevan & Quataert 1998 and references therein).

In this class of accretion solutions the flows are two-temperature with the electron temperature ranging from ≈ 1 MeV in the inner regions to about 1 keV in the outer regions. At these temperatures, and when the gas is optically thin to electron scattering so that Comptonization is unimportant, most of the cooling occurs via thermal bremsstrahlung emission. In recent work it has been shown that the hard X-ray components observed in elliptical galaxy systems (Allen, Di Matteo & Fabian 2000) are indeed consistent with models of thermal bremsstrahlung emission (Di Matteo et al. 2000). In the same work, it has also been emphasized that bremsstrahlung emission may always be the dominant cooling mechanism because hot accretion flows are likely to drive strong mass loss (e.g. Igumenshchev & Abramowicz 1999; Blandford & Begelman 1999) so that their densities and scattering optical depths always remain low and Comptonization is never important. The same also applies to the case in which convection becomes important in hot flows, as discussed in recent work by Narayan, Igumenshchev & Abramowicz (2000), Quataert & Gruzinov (2000), and Ball, Narayan, & Quataert (2000).

The X-ray emission from the nuclei of nearby giant elliptical galaxies is therefore expected to have significantly different properties than that of AGN, reflecting the physical conditions of hot, extended accretion flows. In this paper we go beyond the spectral calculations carried out in earlier work and provide a set of diagnostics of the bremsstrahlung X-ray emitting region of hot accretion flows. This includes calculating the expected surface brightness profiles relevant for determining the sizes and density profiles of the X-ray emitting regions of these flows. The calculations of these quantities may have a significant impact for explaining the ongoing and

upcoming X-ray observations of the cores of galactic nuclei. Conversely, the measurement of these quantities may reveal the relevant mode of accretion and the detailed properties of the accretion flows, improving our understanding of physical processes, such as convection and generation of outflows. Here we discuss the implications of our results for observations with the *Chandra* X-ray Observatory and the proposed future space-based X-ray interferometer *MAXIM*.

In §2, we review bremsstrahlung emission from hot flows and introduce the X-ray diagnostics that we study in this paper. In §3, we present the surface brightness profiles and visibility curves for different black hole masses and accretion-flow density profiles. Finally in §4, we discuss the implications of our results for current and possible upcoming X-ray missions.

2. Bremsstrahlung Emission from Hot Flows

2.1. Advection Dominated Accretion

Optically thin advection-dominated accretion flows (ADAFs) are examples of hot, magnetic plasmas with low radiative efficiency (Ichimaru 1977; Rees et al. 1982; Narayan & Yi 1994, 1995b; Abramowicz et al. 1995; see Narayan et al. 1998 and Kato, Fukue, & Mineshige 1998 for reviews). The dominant emission mechanisms in low mass-accretion rate ADAFs are optically thin bremsstrahlung from the hot electrons, which remain at high temperatures out to large radii in the flow, and synchrotron radiation in the inner regions. Above the mass accretion rates at which the scattering optical depth approaches unity, inverse Comptonization of soft synchrotron photons also becomes important and a Compton peak emerges at X-ray wavelengths. The spectrum of a hot flow around a supermassive black hole, therefore, is characterized by an overall low luminosity, with a synchrotron peak in the radio wavelengths and an X-ray component coming from bremsstrahlung emission, with possible contribution from the Comptonization of soft synchrotron photons in the hot flow. However at the low mass-accretion rates which we consider here, Comptonization is negligible and the X-ray spectra are entirely dominated by bremsstrahlung emission.

In describing these flows, we use dimensionless quantities for the mass, radius, and accretion rate. The black hole masses are given in units of the solar mass, $m \equiv M/M_{\odot}$, and the radii in units of the Schwarzschild radius, i.e., $r \equiv R/R_S$, where $R_S = 2GM/c^2$. We scale the mass accretion rate in units of \dot{M}_{Edd} , i.e., $\dot{m} \equiv \dot{M}/\dot{M}_{\text{Edd}}$, where the Eddington mass accretion rate is $\dot{M}_{\text{Edd}} \equiv L_{\text{Edd}}/\eta_{\text{eff}}c^2$, and η_{eff} is the radiative efficiency taken to be 0.1 for the purposes of this definition.

It has been proposed that mechanisms leading to strong outflows and convection may be common in ADAFs. Outflows have been discussed extensively in the literature (Narayan & Yi 1995a; Igumenshchev & Abramowicz 1999; Blandford & Begelman 1999; Stone, Pringle & Begelman 1999) and have been applied to the spectra of accreting supermassive black holes (Di

Matteo et al. 1999, 2000; Quataert & Narayan 1999). Similarly, convective processes are discussed by Igumenshchev, Chen, & Abramowicz (1996), Narayan, Igumenshchev & Abramowicz (2000), and Quataert & Gruzinov (2000). A simple parametrization of the accretion flow density profile in the presence of outflows was put forth by Blandford & Begelman (1999), in which the mass accretion rate is modified radially and is given by $\dot{m} = \dot{m}_{\text{out}}(r/r_{\text{out}})^p$, where r_{out} is the radius at which the mass accretion rate \dot{m}_{out} is fixed, and $0 < p < 1$ specifies the strength of the outflow. Other processes such as convection may give rise to similar modifications of the radial density profile of these flows. In particular, convective solutions have the same density profiles as the $p = 1$ inflow-outflow solutions although the velocity profile of these solutions differ significantly from that of inflow-outflow solutions (e.g., Narayan et al. 2000). In this paper, we use this parametrization to calculate the electron density profiles which scale as $N_e \propto r^{-3/2+p}$. Throughout this paper, we fix the mass accretion rate \dot{m}_{out} at 10^{-4} at $r_{\text{out}} = 10^5$ unless otherwise specified. The other parameters of the model describing the microphysics are fixed at some typical values: the viscosity parameter $\alpha = 0.1$, the ratio of gas pressure to magnetic pressure $\beta = 10$, and the ratio of viscous electron heating to proton heating $\delta = 10^{-2}$.

In our numerical calculations, we use the global solutions described in Popham & Gammie (1998) to obtain the run of electron temperature and density with radius, with proper modifications of the continuity equation to take into account the changes to the electron density and temperature for $p \neq 0$. These solutions are based on those of Narayan, Kato, & Honma (1997) and Chen, Abramowicz, & Lasota (1997) but include general relativistic effects near the black hole. One caveat in our analysis is that these global solutions are obtained for the $p = 0$ case and this may give rise to errors of order unity for strong outflow cases (see Quataert & Narayan 1999). To make the interpretation of our results more intuitive, we note that the electron temperature is nearly virial and equal to the proton temperature in the outer regions of the flow, but the profile gets flatter at smaller radii ($r \gtrsim 10^3$) due to synchrotron cooling. This gives rise to the two-temperature character of the flow at small radii. The electrons throughout the flow are assumed to be thermal with the Maxwellian energy distribution $N_e(\gamma) = N_e \gamma^2 \beta \exp(-\gamma/\theta) / \theta K_2(1/\theta)$, where γ is the electron Lorentz factor, $\theta = kT/m_e c^2$ is the dimensionless electron temperature, and K_2 is a modified Bessel function.

2.2. Bremsstrahlung Emission

The relativistic electron-proton bremsstrahlung emissivity is given by (Stepney & Guilbert 1983)

$$\frac{dE_{\text{ep}}}{dV dt d\nu d\Omega} \equiv j_{\text{ep}} = \frac{hcN_p}{4\pi} \int_{1+\omega}^{\infty} \omega \frac{d\sigma}{d\omega} \beta N_e(\gamma) d\gamma \quad (1)$$

where for the differential cross-section $d\sigma/d\omega$ we have used the Bethe-Heitler formula derived in the Born approximation (Jauch & Rohrlich 1959). Here, $\omega \equiv h\nu/m_e c^2$ is the dimensionless photon energy, N_p is the proton number density and $N_e(\gamma)$ is the electron density given above. Stepney &

Guilbert (1983) provide fitting functions for the electron-electron bremsstrahlung emissivity given by

$$j_{ee} = N_e^2 \sigma_T \alpha_f m_e c^3 \exp(-x) G(x, \theta) / 4\pi x \quad (2)$$

where σ_T is the Thomson cross-section, α_f is the fine-structure constant, $x \equiv \omega/\theta$, and the fitting function $G(x, \theta)$ can be found in tabular form in Stepney & Guilbert (1983). Typically, $j_{ee} \lesssim 0.1 j_{ep}$ for the frequencies and temperatures considered here.

To calculate the emerging bremsstrahlung intensities, we use a one-dimensional radiative transfer algorithm as described by Özel, Psaltis, & Narayan (2000). We integrate the equation of radiative transfer along plane-parallel rays of varying impact parameters b (perpendicular distances of rays to the central line of sight) through the flow and calculate the emerging intensity (i.e., surface brightness profile) $I(b)$. Note that in our radiative transfer calculations we do not take into account general relativistic redshift and light deflection which will be important for centrally peaked profiles ($p \sim 0$) and may lead to large errors when most of the emission comes from within a few R_S of the event horizon. Our numerical domain extends to an impact parameter of $\sim 10^6 R_S$, beyond which $kT_e \ll 1$ keV and bremsstrahlung radiation does not contribute to the X-ray energies. Also note that our treatment assumes spherical symmetry of the density and temperature profile of the electrons which is a reasonable assumption given that all the flows considered here have large scale heights, with $H/R \approx 1$. For optically thin bremsstrahlung emission in such extended flows, the region around the event horizon, i.e., small radii, have small contribution to the emerging intensity, even at small impact parameters.

2.3. X-ray Diagnostics

The X-ray spectra of hot flows around supermassive black holes have been studied extensively in previous work. Here we consider additional powerful diagnostic quantities that are related to the two primary imaging methods: the brightness profiles of accretion flows, which are directly measurable by single-aperture imaging in X-rays, and the Michelson visibility function, which is the curve measured by an interferometer. Note that two of these diagnostic methods, spectral measurements and CCD imaging, are being carried out with increasing resolution by current X-ray telescopes. Using interferometry to study the sizes and profiles of accretion flows is being planned for future X-ray missions.

The brightness profile $I(b)$ of a spherically symmetric source is the map of the line-integral of the emissivity as a function impact parameter b . To define the visibility function, we first introduce the projected brightness profile $B(x)$. This is defined as the integral of specific intensity in the direction orthogonal to the interferometer baseline; i.e., the aperture spacing vector x (see, e.g., Thompson, Moran, & Swenson 1991) and is given by

$$B(x) \equiv \int I(\sqrt{x^2 + y^2}) dy. \quad (3)$$

Thus $B(x)$ is effectively a surface-integral of the emissivity. The Michelson visibility function is then

$$V_M(k) \equiv \frac{|\int B(x) \exp(ikx) dx|}{|\int B(x) dx|} \quad (4)$$

which is the normalized modulus of the Fourier transform of the projected brightness profile $B(x)$. The visibility function thus probes the characteristic length scales of the flow and can be inverted to give the brightness profile of the source. Finally, the luminosity at each photon frequency for optically thin emission is the volume integral of the emissivity and is a measure of the total energy output from the entire flow at that frequency.

Given the above definitions, we point out that, for optically thin bremsstrahlung emission, the brightness profile, the projected brightness profile, and the luminosity are effectively (but not strictly) the three radial moments of bremsstrahlung emissivity j . Because of this, as well as due to the strong dependence of bremsstrahlung emissivity j on electron density ($j \propto n^2$), intensity I_ν and projected brightness profile B_ν are strong indicators of the density profiles of the hot flows.

3. Results: Intensity and Visibility

Figure 1 shows the emerging intensity at 1 and 10 keV as a function of impact parameter for a hot accretion flow around a $10^9 M_\odot$ black hole. The solid curves show the intensity profile at 1 keV while the dashed curves correspond to 10 keV. As expected from the dependence of intensity on the density profile, flows with strong winds or convection ($p=1$) have flat radial intensity profiles extending up to the radii at which the electron temperature drops below 1 and 10 keV, corresponding to $r \sim 10^6$ and $r \sim 10^5$ respectively. The profiles steepen significantly as the parameter p decreases, with the steepest profile corresponding to the case with no outflows. The 10 keV emission is suppressed overall with respect to the 1 keV emission and cuts off exponentially at ≈ 0.1 of the radius of the 1 keV emitting region. This is because the temperature is nearly virial at these radii and order of magnitude difference in temperature corresponds to roughly the same difference in r . Finally, we note that since the hot flows show self-similar behaviour, the intensity *profile* does not change with changing black hole mass, even though the normalization of the intensity scales with mass.

The *extent* and *size* of hot accretion flows show significantly different responses to changing outflow strength. By size, we mean the full-width half maximum (FWHM) of the visibility curve, while by extent we refer to the radius marking the exponential cutoff of emissivity (full-width zero intensity). The full-width zero intensity is very insensitive to p ; irrespective of the steepness of the density profiles, all flows extend out to large radii before the exponential cut-off. However, the steepness of the brightness profiles changes dramatically, with most of the emission arising from within $\sim 6R_S$ for $p = 0$ and within $10^4 R_S$ for $p = 1$ (Figure 1). Therefore, the corresponding sizes also change by orders of magnitude (see Figure 2).

Figure 2 shows the Michelson visibility curves as a function of angular wavenumber $k_\theta = 1/\theta$, where θ is the angular size of the X-ray region in arcseconds. The top axis shows the corresponding baseline needed to resolve a scale k_θ at 1 keV. The dashed lines are the visibility functions for a $10 M_\odot$ galactic black hole at 3 kpc distance, while the solid curves show the case for a $10^9 M_\odot$ black hole at 18 Mpc (Virgo cluster) distance. Both of these are plotted for different outflow strengths, $p = 0, 0.5$, and 1. Finally, as a specific example, we plot with the dotted line the visibility function for a hot accretion model of M87, with a density profile that best fits the observed spectrum of this source (with $\dot{m}_{\text{out}} = 0.015$, $r_{\text{out}} = 300$, $p = 0.45$, Di Matteo et al. 2000).

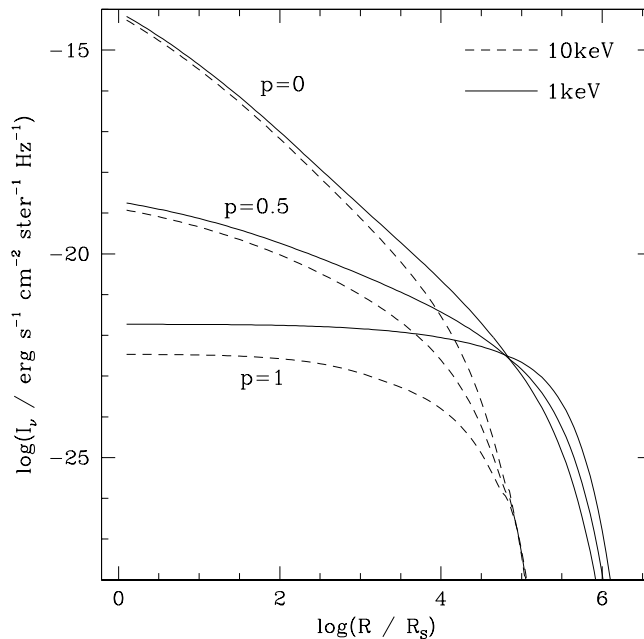


Fig. 1.— The surface brightness as a function of impact parameter in units of Schwarzschild radius R_S for three values of the outflow parameter $p = 0, 0.5$, and 1 for a black hole mass $m = 10^9$. The solid lines shows the bremsstrahlung intensities at 1 keV, while the dashed lines correspond to 10 keV.

The typical observed angular sizes of these flows range from $\sim 0.01 - 1$ arcsec for the case of the supermassive black hole and from $1 - 100 \mu\text{arcsec}$ for the galactic black hole. This is in accordance with the profiles shown in Figure 1, which shows that the characteristic angular size of the bremsstrahlung emitting region increases significantly in the presence of an outflow. Specifically, for strongly modified density profiles ($p = 1$), the flow sizes are large, typically corresponding nearly to their whole extent, $10^6 R_S$. This is because the intensity profile is flat and therefore the only characteristic scale in the flow is the size of the entire 1 keV emitting region. On the other hand, for intensities that are radially peaked, i.e., when $p \lesssim 0.5$, the power is distributed over a broader range of scales and the characteristic size of the flow is smaller. Specifically, a purely inflow ADAF is extended but still centrally peaked, with a measurable FWHM of only tens

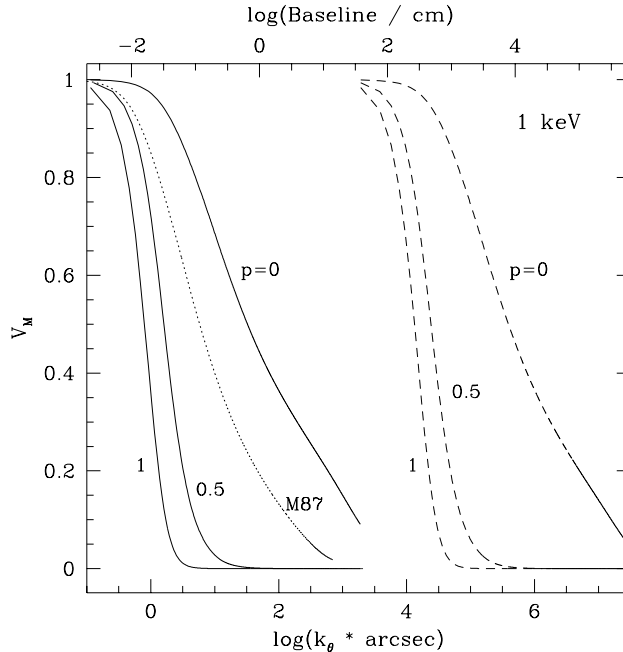


Fig. 2.— The solid lines show the Michelson visibility curves for a $10^9 M_\odot$ black hole at a distance of the Virgo cluster (18 Mpc) for $p=0, 0.5$, and 1. The dashed curves correspond to a $10 M_\odot$ black hole at 3kpc distance. The dotted line is the visibility function for a specific model of M87 with a density profile that best fits the observed spectrum of this source (Di Matteo et al. 2000). The bottom axis shows the angular wavenumber in units of inverse arcseconds while the top axis shows the baseline that would be required for resolving a wavenumber k_θ at 1keV.

of R_S (for the $p = 0$ case, $\text{FWHM} = 30$).

The complementary nature of the two imaging methods, namely imaging which probes directly the intensity profiles, and interferometry which measures the visibility function, is evident in Figures 1 and 2. The extended flows around supermassive black holes with flat profiles have large characteristic angular sizes extending up to 1 arcsec, which may be resolved with direct imaging instruments (see §4 for a discussion of specific instruments). On the other hand, an interferometer with a baseline of $\gtrsim 1m$ is not sensitive to most of the power on large scales and is thus not suitable to study these flows. Furthermore, since the flat density profile flows are also less luminous, it is advantageous to observe these sources with direct imaging instruments which, unlike an interferometer, allow for a photon-energy integrated signal. The situation, however, is reversed for flows with radially peaked intensity profiles. Here, a good resolution that is necessary to study the characteristic sizes of a few tens of R_S can be achieved only by an interferometer. Therefore, both interferometric and direct imaging studies are needed to study the varying characteristics of hot accretion flows. In §4, we discuss further the resolution requirements for upcoming instruments which would allow the current direct imaging instruments and interferometry to work in this complementary manner.

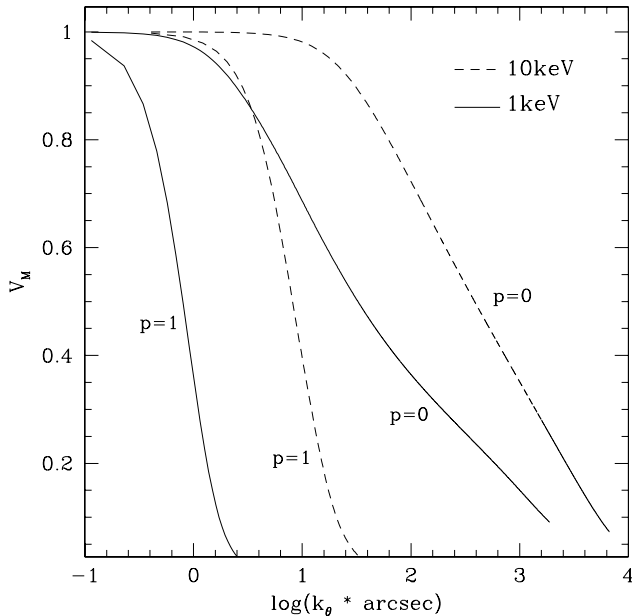


Fig. 3.— The change in the visibility functions from 1 keV to 10 keV for a black hole mass $m = 10^9$ and $p=0$ and 1. Both the sizes of the flow and the visibility functions depend strongly on photon energy.

In Figure 3, we show the change in the visibility function from 1 keV to 10 keV. The characteristic size of the 10 keV emitting region decreases by an order of magnitude for both $p = 1$ and $p = 0$. Furthermore, since the 10 keV brightness profile falls off more steeply in radius for $p < 1$ (Fig.1), the visibility functions are broader.

4. Discussion

High resolution X-ray imaging and interferometric studies, which measure directly or indirectly the brightness profiles and thus the sizes and density profiles of accretion flows around black holes, can be powerful probes for studying the relevant mode of accretion and the detailed properties of accretion flows. We have shown that the 1 keV emitting regions of hot accretion flows can be large and extend up to $10^6 R_S$ irrespective of the specifics of the density profile, provided that the ADAF itself extends out to this radius (see below for further discussion). However, the brightness profiles and visibility functions are strongly affected by the specific density profile. In particular, the flat density profiles in the presence of strong outflows ($p=1$) give rise to very flat surface brightness profiles with characteristic sizes of $10^6 R_S$. In contrast, the purely inflow advection dominated solutions have centrally peaked profiles with characteristic sizes of only a few tens of R_S .

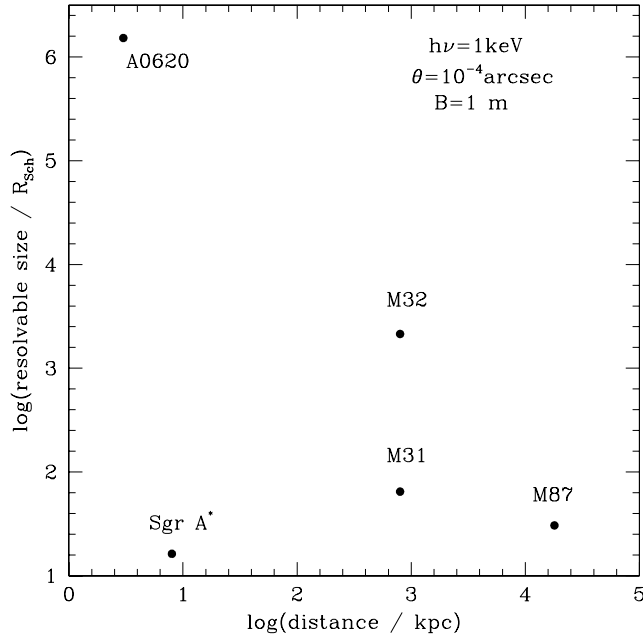


Fig. 4.— The resolvable scale in units of R_S of each source plotted against the known distance to the sources. If the black holes are accreting via a hot flow, these resolvable sizes represent the largest size the accretion flow can have to be resolved by a *minimum* baseline of 1m.

If we are correct in surmising that hot accretion flows may be common in nearby galactic nuclei and that such flows may drive strong outflows (e.g., Quataert & Narayan 1999; Di Matteo et al. 2000) then the above results have strong implications for X-ray observations of these nuclei. An important consequence of our results is that a hot accretion flow with a flat density profile around a $\sim 10^9 M_\odot$ black hole at Virgo cluster distances, such as M87, may look like an extended X-ray source rather than a point source when imaged by the *Chandra* X-ray observatory with its 0.5 arcsec resolution mirrors. At the distance of M87 and for $m \sim 3 \times 10^9$ (Macchetto et al. 1997), 0.5 arcsec corresponds to $10^5 R_S$ which is about an order of magnitude smaller than the extent of the regions of these flows emitting soft X-rays (at $\lesssim 2$ keV; where most of the photon counts would be at these fluxes). Conversely, the detection of an X-ray point source in elliptical nuclei in Virgo must imply that either the physical sizes of the hot accretion flows are smaller than $10^5 R_S$ or that standard thin disk accretion with its associated corona applies. Regarding the former possibility, we stress that in our calculation we have assumed that the hot flows extend to their maximum possible X-ray emitting radius, i.e., $R \sim 10^6 R_S$. This radius is consistent with the typical accretion radius (the radius at which the black hole gravitational potential dominates that of the galaxy) of elliptical galaxies (~ 0.1 kpc; Di Matteo et al. 2000) but does not need to coincide with the radius at which the angular momentum dominated accretion flow, i.e. an ADAF, is formed. There may be physical processes such as cooling at large radii that may cause the ADAF flow to start

at smaller radii, or there may be transitions to other accretion solutions in the outer regions (see, e.g., Igumenshchev, Abramowicz, & Novikov 1998; Menou et al. 1999). Here, we assumed a direct transition from the hot interstellar medium (ISM) of the elliptical galaxies to an ADAF.

We note also that this hot ISM of the elliptical galaxies, with typical temperature of a few keV, may also contribute significantly to the emission in the soft X-ray band, which would further blend the images and may make the detection of the accretion flow component more difficult. However, in the hard band (> 5 keV), the sources are intrinsically smaller (c.f., Fig. 3), and may look more point-like provided that there are enough photon counts. This would have the additional advantage of having less background from galactic emission. Finally, we stress that *Chandra* X-ray spectroscopy of the central regions of these galaxies will also complement the information provided by the imaging instruments and will be crucial for determining the presence of ADAFs in these systems. With its 1 MeV temperature, the bremsstrahlung emission from the central regions of a hot accretion flow will be much harder than that of the galaxy ISM and will have a different spectral slope than that expected from a typical AGN with low luminosity.

Variability studies are also important for determining the sizes of accretion flows and are complementary to imaging studies. Rapid variation in the X-ray flux may help constrain the size of the X-ray emitting region. For example, *ROSAT* HRI observations (at $E \sim 1$ keV) of the “core” of M87 show $\approx 20\%$ variability on timescales of ≈ 6 months to a year (Harris, Biretta, & Junor 1997). This is not easy to reconcile with a $p > 0.5$ bremsstrahlung model for the X-ray emission. However, identifying the possible contributions to the variability from jets associated with the accretion flows relies on high resolution imaging studies and therefore the two methods can be used as complementary probes.

Because of the large inferred black hole masses, many of the nearby supermassive black holes have also been considered some of the best targets for observations with the planned X-ray interferometry mission *MAXIM*. Owing to the short X-ray wavelengths, remarkably high spatial resolutions can be achieved with relatively short baselines with the ultimate aim of imaging of black holes on even horizon scales. (See <http://maxim.gsfc.nasa.gov/> for a detailed discussion of the proposed capabilities of *MAXIM* and Cash et al. 2000). Already for the first stages of such a mission, a target resolution of 0.1 mas has been planned corresponding to a baseline of ~ 1 m at 1 keV. This should probe up to a few tens of R_S for the supermassive black holes in nearby galaxies (Fig 4).

However, if indeed large black holes in nearby galaxies accrete via hot, radiatively inefficient accretion flows, e.g. M87, one important consequence of our results is that characteristic X-ray emission scale would be large and there would be little power on scales corresponding to few tens of R_S or smaller. Therefore baselines of ~ 1 m may not be appropriate to image black holes in the Virgo ellipticals (c.f., §3 and Fig. 2) and a range of smaller baselines would be necessary to study the visibility functions of these extended flows. Thus, to study properties of accretion flows, the minimum baseline of the interferometer is an important consideration. Specifically, for studying

the spatial extent of hot accretion flows and the relevance of outflows, it is important to bridge a possible gap in resolution between that of the *Chandra* X-ray observatory and the minimum resolution of an X-ray interferometer. Alternatively, with a baseline of ~ 1 m, galactic black hole candidates may be better targets to study hot accretion flows (Fig. 2). *Chandra* observations will be crucial for selecting the appropriate targets for an X-ray interferometry mission and giving us clues on the relevant mode of accretion in the nearby black holes.

We thank Ramesh Narayan for many useful suggestions throughout this work. We also thank Dimitrios Psaltis, Martin White, Irwin Shapiro, and George Rybicki for valuable discussions and comments on the manuscript. T.D.M. acknowledges support for this work provided by NASA through Chandra Postdoctoral Fellowship grant number PF8-10005 awarded by the Chandra Science Center, which is operated by the Smithsonian Astrophysical Observatory for NASA under contract NAS8-39073. This work was supported in part by NSF Grant AST 9820686.

REFERENCES

- Abramowicz, M. A., Chen, X. , Kato, S. , Lasota, J. -P. & Regev, O. 1995, ApJ, 438, L37
- Allen, S. W., Di Matteo, T., & Fabian, A. C. 2000, MNRAS, 311, 493
- Ball, G., Narayan, R., & Quataert, E., 2000, ApJ, submitted (astro-ph/0007037)
- Blandford, R. D. & Begelman, M. C. 1999, MNRAS, 303, L1
- Cash, W., Shipley A., Osterman, S., Joy, M., 2000, Nature, 407, 160
- Chen, X. , Abramowicz, M. A. & Lasota, J. -P. 1997, ApJ, 476, 61
- Di Matteo T., Fabian A.C., Rees M.J., Carilli C.L., Ivison R.J. 1999, MNRAS, 305, 492
- Di Matteo, T., Quataert, E., Allen, S. W., Narayan, R., & Fabian, A. C. 2000, MNRAS, 311, 507
- Fabian A. C., Rees M. J., 1995, MNRAS, 277, L55
- Eckart, A. & Genzel, R. 1997, MNRAS, 284, 576
- Haardt, F. Maraschi, L. 1991, ApJ, 380, L51
- Haardt, F. Maraschi, L. 1993, ApJ, 413, 507
- Harris, D. E., Biretta, J. A. and Junor, W. 1997, MNRAS, 284, L21
- Ichimaru, S. 1977, ApJ, 214, 840
- Igumenshchev, I. V. Abramowicz, M. A. 1999, MNRAS, 303, 309

- Igumenshchev, I. V., Abramowicz, M. A. and Novikov, I. D. 1998, MNRAS, 298, 1069
- Igumenshchev, I. V., Chen, X. Abramowicz, M. A. 1996, MNRAS, 278, 236
- Jauch, J. M. Rohrlich, F. 1959, Theory of Photons and Electrons (New York: Springer)
- Kato, S., Fukue, J. & Mineshige, S. 1998, Black-hole Accretion Disks (Kyoto: Kyoto University Press)
- Macchetto, F., Marconi A., Axon D.J., Capetti A., Sparks W., Crane P., 1997, ApJ, 489, 579
- Magorrian, J. , et al. 1998, AJ, 115, 2285
- Menou, K., Esin, A. A., Narayan, R., Garcia, M. R., Lasota, J. and McClintock, J. E. 1999, ApJ, 520, 276
- Nandra K., George I.M., Mushotzky R.F., Turner T.J., Yaqoob T., 1997, ApJ, 477, 602
- Narayan R., Igumenshchev I. V., Abramowicz M. A. 2000, ApJ, 539, 798
- Narayan, R. , Kato, S. & Honma, F. 1997b, ApJ, 476, 49
- Narayan, R., Mahadevan, R. & Quataert, E. 1998, in Theory of Black Hole Accretion Disks, Eds. M. Abramowicz, G. Bjornsson, and J. Pringle (Cambridge: Cambridge University Press)
- Narayan, R. , McClintock, J. E. Yi, I. 1996, ApJ, 457, 821
- Narayan, R. & Yi, I. 1994, ApJ, 428, L13
- . 1995a, ApJ, 444, 231
- . 1995b, ApJ, 452, 710
- Narayan, R., Yi, I. Mahadevan, R. 1995, Nature, 374, 623
- Özel F., Psaltis D., Narayan R., 2000, ApJ, 541, 234
- Popham, R. & Gammie, C. F. 1998, ApJ, 504, 419
- Quataert E., Gruzinov A., 2000, ApJ, 539, 809
- Quataert E., Narayan R., 1999, ApJ, 520, 298
- Rees M. J., Begelman M. C., Blandford R. D., Phinney E. S., 1982, Nature, 295, 17
- Stepney, S. Guilbert, P. W. 1983, MNRAS, 204, 1269
- Stone, J. M., Pringle, J. E. Begelman, M. C. 1999, MNRAS, 310, 1002

Thompson, A. R. , Moran, J. M. Swenson, G. W. 1991, Interferometry and Synthesis in Radio Astronomy (Malabar: Krieger)